ACS NANO
Cite This: ACS Nano 2018, 12, 1482−1490
www.acsnano.org

ARTICLE

Proteolytic Nanoparticles Replace a Surgical Blade by Controllably Remodeling the Oral Connective Tissue

Assaf Zinger,[†] Omer Adir,[†] Matan Alper,[†] Assaf Simon,[†] Maria Poley,[†] Chen Tzror,[†] Zvi Yaari,[†] Majd Krayem,[†] Shira Kasten,[†] Guy Nawy,[†] Avishai Herman,[†] Yael Nir,[†] Sharon Akrish,[‡] Tidhar Klein,[§] Janna Shainsky-Roitman,[†] Dov Hershkovitz,[∥] and Avi Schroeder*[,†]

[†]Department of Chemical Engineering, Technion−Israel Institute of Technology, Haifa 32000, Israel
[‡]Department of Oral and Maxillofacial Surgery, Rambam Medical Center, Haifa 3109601, Israel
[§]Moriah Animal Companion Center, Haifa 32762, Israel
[∥]Department of Pathology, Tel Aviv Sourasky Medical Center, Tel Aviv 62431, Israel

Supporting Information

ABSTRACT: **Surgical blades are common medical tools. However, blades cannot distinguish between healthy and diseased tissue, thereby creating unnecessary damage, lengthening recovery, and increasing pain. We propose that surgical procedures can rely on natural tissue remodeling tools—enzymes, which are the same tools our body uses to repair itself. Through a combination of nanotechnology and a controllably activated proteolytic enzyme, we performed a targeted surgical task in the oral cavity. More specifically, we engineered nanoparticles that contain collagenase in a deactivated form. Once placed at the surgical site, collagenase was released at a therapeutic concentration and activated by calcium, its biological cofactor that is naturally present in the tissue. Enhanced periodontal remodeling was recorded due to enzymatic cleavage of the supracrestal collagen fibers that connect the teeth to the underlying bone. When positioned in their new orientation, natural tissue repair mechanisms supported soft and hard tissue recovery and reduced tooth relapse. Through the combination of nanotechnology and proteolytic enzymes, localized surgical procedures can now be less invasive.**

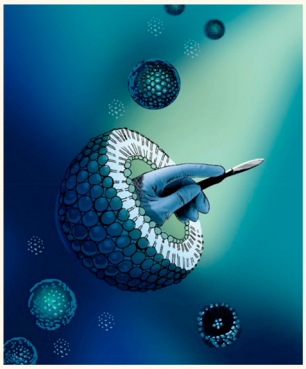

KEYWORDS: *nanotechnology, protein delivery, extracellular matrix, liposomes, collagen, biosurgery*

Five million patients undergo orthodontic procedures annually in the U.S. alone.[1] In cases of severe malocclusion, a minor surgical intervention is necessary in order to maneuver the teeth to their proper position (Figure 1A).[2] During this procedure, collagen fibers that connect the teeth to the underlying alveolar bone are sectioned with a scalpel (Figure 1B). After the surgery, braces are used to maneuver the teeth to their proper orientation. Despite the potential benefits of surgery, many patients opt not to undergo such procedures due to their invasive nature. Here, we tested the ability of nanoparticles loaded with a proteolytic enzyme to replace such procedures by directly targeting collagen type-I fibers in the oral cavity (Figure 1C).

There are 28 types of collagens in the human body that are tuned for the mechanoelastic function of each organ. In the oral space (specifically in the gingiva), collagen type-I supracrestal fibers connect between the teeth and the alveolar bone. During orthodontic procedures, tooth movement depends on remodeling of the supracrestal collagen fibers and bone.[3] This force-induced process can be painful[4] and, for its successful completion, requires that the collagen fibers remodel in line with the final positioning.[5]

Collagenase is a matrix metalloproteinase which is naturally in control of biodegrading collagen in the extracellular matrix[6] and a key player in tissue remodeling processes.[7] Collagenase is clinically approved for digesting abnormal thickening of the skin and tissues of the palms in patients suffering from Dupuytren's contracture.[8] In order to prevent damage to collagen-containing tissues that surround the treatment site, the enzyme concentration and spatial biodistribution must be carefully controlled.

Nanotechnologies promise to revolutionize medical care by improving accuracy and targeting therapeutics to the disease site.[9−11] To date, more than 80 nanotechnologies have been approved for clinical use.[12,13] Liposomes, nanoscale vesicles with an inner aqueous core that is surrounded by a lipid bilayer

Received: November 10, 2017
Accepted: January 24, 2018
Published: January 24, 2018

DOI: 10.1021/acsnano.7b07983
ACS Nano 2018, 12, 1482−1490

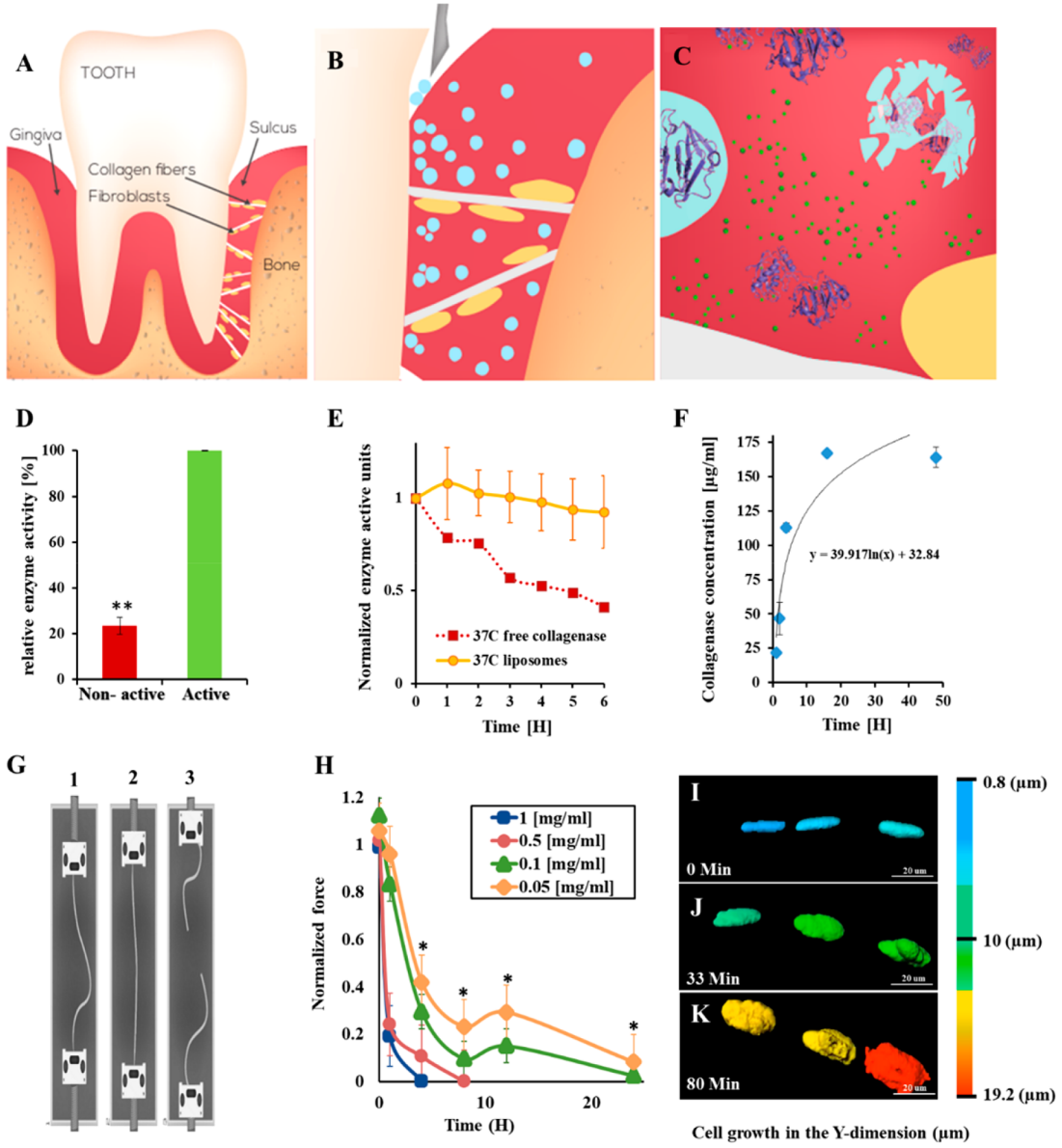

Figure 1. Nanosurgery: enzymes loaded into nanoparticles are released at the surgical site, where they are activated, to perform a localized surgical task. Proteolytic enzymes, housed within nanoparticles replace the traditional blade, thereby cutting only the target tissue, reducing pain and enhancing recovery. We utilized this approach to replace a surgical procedure in the oral tissue. Teeth are confined to their natural orientation by soft and hard tissue (A). Specifically, collagen type-I fibers anchor the teeth to the underlying bone. Nanoparticles (blue spheres) loaded with collagenase, a proteolytic enzyme with specificity toward collagen, are inserted into the sulcus (B). The particles house the enzyme in a deactivated form. Once released, Ca^{2+} ions, naturally present in the tissue, activate the enzyme and collagen degradation begins. The nanoparticles maintain the enzyme's therapeutic release profile and confine the biodistribution to the treatment site. (C) This facilitates enhanced orthodontic tooth movement. The collagen fibers recover rapidly after the treatment. Illustrated by Bonnie Manor. Controlled release and activation. Collagenase released from the nanoparticles over 48 h at physiological conditions (F). Once released, the enzyme is activated by its cofactor calcium, naturally present in the tissue (D). The activity of the collagenase declines thereafter, over a period of 6 h (E). As long as the enzyme is housed inside the particle, it remains protected and inactive (D and Supplementary Figure S8A,B). Collagenase relaxes collagen fibers. Collagen fibers were exposed to collagenase at various concentrations for different periods of time. The fibers were stressed using a force machine under oral physiological conditions (G and Supplementary Figures S3 and S8C), illustrated by Dima Zagorski. As the collagenase concentration increased, the fibers weakened (H). The higher collagenase concentrations (0.5 and 1 mg/mL) degraded the collagen fibers within less than 10 h. A therapeutic window of 0.05−0.1 mg/mL at which the collagen fibers were relaxed but not fully degraded by collagenase was determined. Fibroblast morphology changes as a function of collagenase activity. A collagen fiber (beneath the optical field) with adherent fibroblasts in focus was imaged during the process of collagenase treatment. As the collagen fiber relaxes, the adherent fibroblasts change their morphology from an elongated structure to a round structure (I→J→K, collagenase was added at t = 0). A full time-lapse movie of the process is presented at https://youtu.be/4krwecUS7Yc. It is important to note that the collagenase relaxed the collagen fibers but did not detach the fibroblasts nor impact their viability. Error bars indicate the standard deviation of at least five independent measurements; *denotes a two-tailed p value <0.05; **denotes a two-tailed p value <0.01.

membrane, are clinical drug delivery systems.[14] Tailoring the liposome size and composition modulates biodistribution and controls the drug release profile at the target site.[15] For example, liposomes are used for targeting anticancer agents to

DOI: 10.1021/acsnano.7b07983
ACS Nano 2018, 12, 1482−1490

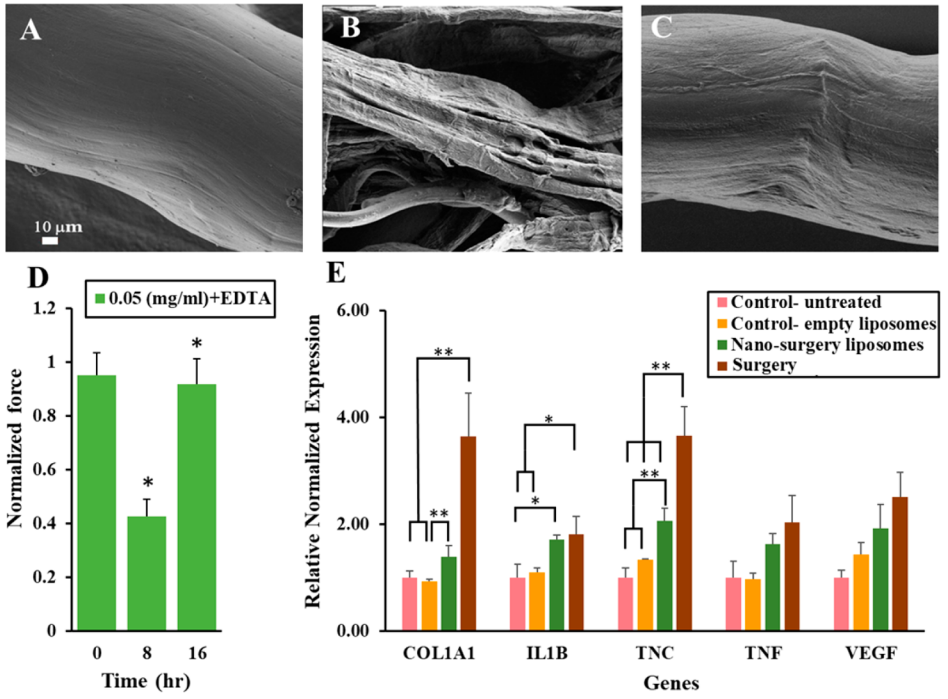

Figure 2. Collagen regeneration. A collagen fiber was imaged using high-resolution scanning electron microscope before (A), during (B), and after being exposed to collagenase, allowing collagen regeneration (C). Collagen relaxation and regeneration. Collagen fibers were stressed using a force machine. Strength measurements were performed before adding the collagenase, during the collagenase disassembling activity, and 16 h after the collagenase activity was retarded. The collagen fibers regained ~90% of their initial strength profile (D). All data points are the mean of 14−20 experiments. Regenerative genes are upregulated at the treatment site. Collagenase type-I was inserted into rat's sulcus, *in vivo*. Twenty-four hours later, the tissue surrounding the teeth was collected, and RNA was isolated (E). The RNA profile of Col1A1, IL1b, TNC, VEGF, and TNFα (genes associated with collagen repair and extracellular matrix remodeling) was measured. The β-2 microglobulin (B2M) was used as the relative housekeeping gene; *indicates a two-tailed unequal variance p value of <0.05; **indicates a two-tailed unequal variance p value of <0.01. A one-way ANOVA analysis of gene expression comparing between the enzymatic nanosurgery group, the untreated, and the empty liposome treatment groups, demonstrated a significant effect of the liposome surgery on gene expression, having a $p < 0.05$ for the COLA1A1 gene [$F(3,15) = 9.05$, $p = 0.001$], IL1B gene [$F(3,16) = 7$, $p = 0.003$], and TNC gene [$F(3,16) = 32.9$, $p < 0.001$]. Post hoc comparisons using the Benjamini−Hochberg procedure using an error discovery rate of $Q = 10\%$ indicated that for the COLA1A1 gene the mean score of nanosurgery group plus braces ($M = 2.3$, SD = 0.6) was significantly different than that of the control empty liposome group ($M = 0.64$, SD = 0.16). However, it did not significantly differ from the control untreated group ($M = 1$, SD = 0.07). For the IL1B gene, the mean score of nanosurgery group plus braces ($M = 2.5$, SD = 0.5) was significantly different than that of the control untreated group ($M = 1$, SD = 0.2) and the control empty liposomes group ($M = 1.1$ SD = 0.1). For the TNC gene, the mean score of nanosurgery group plus braces ($M = 2.2$, SD = 0.2) was significantly different than that of the control untreated group ($M = 1$, SD = 0.1) and the control empty liposome group ($M = 1.3$ SD = 0.01).

tumors or for the localized controlled-release of analgesics. However, the delivery of enzymes from liposomes remains a challenge.[16]

In this study, we developed a drug delivery system that releases the proteolytic enzyme collagenase type-I to remodel collagen-I fibers in the oral space, to replace a minimal surgery performed in the oral space.

RESULTS AND DISCUSSION

Collagenase Nanoparticles Inhibit Early Activation of the Enzyme. Collagenase is a proteolytic enzyme that cleaves the collagen backbone by detaching the peptide bond between glycine and leucine or isoleucine.[17] We chose to work with collagenase type-I to relax the supracrestal collagen-I fibers that connect the teeth to the underlying alveolar bone.

Collagenase is activated by calcium, its biological cofactor, which catalyzes the proper folding of the enzyme and enables collagenase binding to its collagen substrate (Figure 1D). Once activated, the half-life of collagenase is several hours until it is retarded by metalloproteinase inhibitors or by other physiological conditions (Figure 1E). We sought to develop a system in which collagenase is activated only after it is placed at the surgical site. For this, we loaded collagenase into the 100 nm liposomes in the absence of Ca. The liposomal lipid bilayer, composed of 1,2-dimyristoyl-*sn*-glycero-3-phosphocholine (DMPC), is impermeable to Ca^{2+} ions (Figure 1E).[18] This impermeability protects the enzyme from early activation (Figure 1D,E). The liposome lipids were not susceptible to degradation by collagenase (Supplementary Figure S1). Once placed in the sulcus, collagenase began diffusing out of the liposomes (Figure 1F and Supplementary Figure S2). Naturally present in the oral cavity, the calcium activated the enzyme, which in turn began relaxing the collagen fibers (Figure 1G,H).

Collagenase Relaxes Collagen Fibers in a Concentration-Dependent Manner.[19] More than 300 collagen fibers were stressed in the presence of collagenase at different concentrations using an experimental setup that mimics the physiological conditions (Figure 1G). The tensile strength of each collagen fiber was measured as a function of the collagenase concentration and treatment time.

As the concentration of collagenase increased, the fibers weakened (Figure 1H). During this process, a therapeutic

DOI: 10.1021/acsnano.7b07983
ACS Nano 2018, 12, 1482−1490

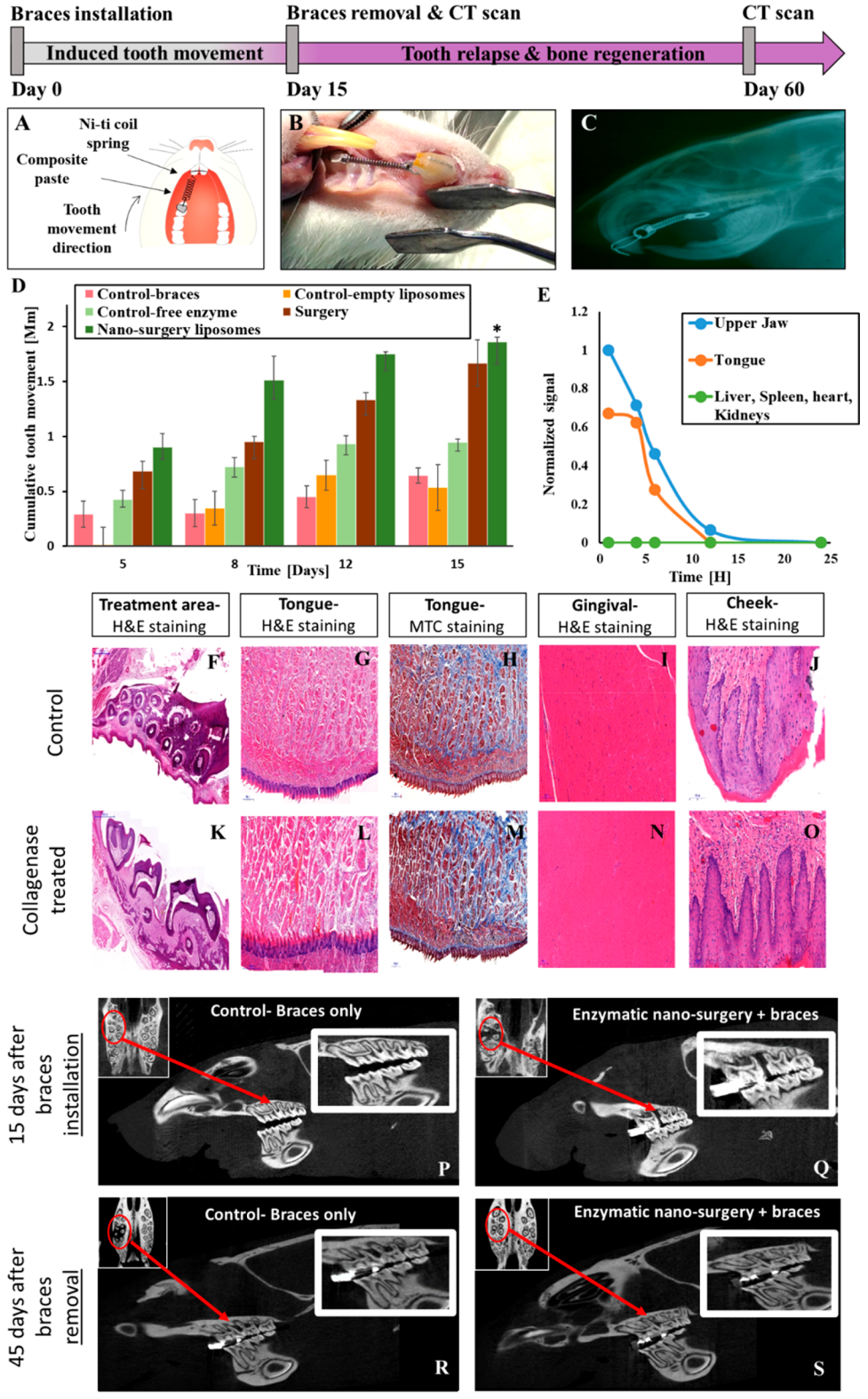

Figure 3. Accelerating orthodontic treatments with a local application of enzymes. Nanoparticles containing a therapeutic dose of collagenase (0.2 mg/mL) were inserted into the sulcus of Wistar rats. An orthodontic spring was used to connect the front upper right molar to the incisors, generating a constant pull force of 2 N (A, schematic; B, photograph), illustrated by Rohan Aggarwal. A lateral X-ray scan of a Wistar rat with an orthodontic spring connecting the front upper right molar to the incisors generated a constant pull force of 2 N (C). The gap between the front incisors and molar was measured over time using a caliper and the effect of the procedure on the underlying tissue was evaluated. Tooth displacement was measured over a period of 15 days with and without nanosurgery or in comparison to oral surgery. Three test groups consisted of rats treated with nanoscale liposomes, free enzyme, or oral surgery. Two control groups consisted of rats with braces only or a sham treatment with empty liposomes (D). *One-way ANOVA analysis, comparing tooth movement in the nanosurgery group plus braces *versus* braces alone, or to the free enzyme plus braces, or the empty liposomes (sham) plus braces, demonstrated a significant effect of $p < 0.05$ in all four conditions $[F(4,19) = 3.78, p = 0.01]$. Post hoc comparisons using the Benjamini–Hochberg procedure using error discovery

DOI: 10.1021/acsnano.7b07983
ACS Nano 2018, 12, 1482–1490

Figure 3. continued

rate of Q = 10% indicated that the mean score of nanosurgery group plus braces (M = 1.86, SD = 0.16) was significantly different than the braces group (M = 0.64, SD = 0.16). However, it did not significantly differ from the surgery group (M = 1.66, SD = 0.26). Liposome biodistribution. The biodistribution of nanoliposomes was tracked. Organs were collected at different time points with the highest fluorescent levels measured at the treatment site (E). After 4 h, a 50% decrease in the signal was recorded. After approximately 12 h, the signal was below detection (Supplementary Figure S9). Histological evaluation of collagenase-treated tissues. Seven days after placing the collagenase liposomes in the rat sulcus, oral tissues of the control (G−J) and treated (L−O) groups were stained with H&E and Masson's trichrome. Both histological groups appear similar; specifically, no difference was noticed between the control to the treated group after 15 days of treatment surrounding the treatment area (F,K). Bone regeneration after nanosurgery: Hard and soft tissue regeneration is imperative for surgical recovery. We compared bone regeneration with and without the enzymatic nanosurgery. Liposomal collagenase was placed in the rat's upper right molar sulcus together with an orthodontic spring, among the test group for 15 days. Lateral and axial views of the control (braces only) (P) and nanosurgery (Q) groups were imaged by microCT on day 15. The tooth enhanced movement can be noticed between the front and second molars and is marked with red circles and arrows. Full bone regeneration was observed 60 days after initiating the treatment (45 days after removing the braces) in the nanosurgery group (S) but not in the normal orthodontic group (R).

collagenase concentration of 0.05−0.1 mg/mL was determined, at which the fibers relaxed but did not tear. We expressed the relative change in fiber strength during the treatment using a dimensionless number, α:

$$\alpha = \frac{\text{force needed to tear a collagenase-treated fiber}}{\text{force needed to tear an untreated fiber}}$$

A descending α slope implies that the collagen bundle is weakening, while an ascending slope implies that a reparative process is occurring. Three modes of α can be noticed, as the collagen bundles are being exposed to collagenase (Figure 1H and Supplementary Figure S3). At first, rapid weakening of the fibers treated with collagenase was recorded ($1 < \alpha < 0.2$). Thereafter, some strengthening of the collagen fibers occurred ($0.2 < \alpha < 0.4$) followed by gradual collagen weakening until the fiber tore ($\alpha = 0$). The weakening of the collagen is intuitive due to the degradative activity of the collagenase. However, the strengthening of the fiber suggested that endogenous collagen repair mechanisms are activated after the fiber is exposed to collagenase.

Fibroblasts Remain Adherent to the Collagen Fiber throughout the Treatment, Secreting Tissue Remodeling Factors and Initiating Collagen Repair.[20] Fibroblasts play an important role in collagen remodeling.[21] Adherent to the collagen fibers, fibroblasts sense the fiber tension and initiate regenerative processes when the fiber is degraded. Using a time-lapse laser scanning confocal microscopy, we imaged the fibroblast morphology in response to the collagenase treatment (Figure 1I−K). When the fiber was stretched, the fibroblasts had an elongated, ellipse morphology (Figure 1I). Due to the exposure to collagenase, the fiber relaxed and the fibroblasts assumed a round structure (Figure 1J,K; a time-lapse movie of the morphological change in the adherent fibroblasts can be see at https://youtu.be/4krwecUS7Yc). Interestingly, throughout the process, we did not observe fibroblast detachment from the fiber, and fibroblast viability was retained (Figure 1I−K). This finding suggests that natural reparative processes can be carried out by the adherent fibroblasts (Figure 2).

Collagen Regeneration. Using collagen type-I fibers sourced from a rat, we were able to observe the regenerative process after the enzymatic treatment (Figure 2A−C). The mechanical properties of the collagen fibers were tested before, during, and after the exposure to collagenase (Figure 2D). The tensile strength of the collagen fibers was approximately 5 N before being exposed to collagenase. After the fibers were exposed to a therapeutic dose of collagenase, their strength decreased by approximately 50%. As expected, 16 h after completing the process, the fibers regained their initial strength (Figure 2D).

Throughout the treatment, we imaged the morphological changes that the collagen fiber undergoes using scanning electron microscopy (Figure 2A−C). Before the treatment, we observed that the collagen has a tightly packed fiber structure. After being treated with collagenase, the collagen fibers unraveled (Figure 2A). Several hours after retarding the collagenase activity, collagen fibers resumed their initial morphology (Figure 2B) with the exception of some regions of the regenerated fiber which were not perfectly aligned (Figure 2C). There is a slight discrepancy between the time it takes the fiber to reach visual repair (as seen under the electron microscope) and mechanical repair (as measured using a force machine). Even though the fiber appears regenerated, the internal molecular bonds between the collagen bundles may require more time to fully develop.

Collagen-Repairing Genes Are Activated Following the Procedure. Regenerative biological cascades were triggered in response to the degradative signal. We applied collagenase type-I to rat's gingiva, *in vivo*. Twenty-four hours later, the tissue surrounding the teeth was collected and RNA was isolated. The RNA profile of genes that are associated with collagen repair and extracellular matrix remodeling was measured (Figure 2E). We found that multiple genes were upregulated in the treated tissue, namely, Col1a1, a gene that encodes for collagen type-I synthesis, IL1B, a gene that is associated with osteoclast activation, and TNC, a gene that is expressed during remodeling of the extracellular matrix (Figure 2E).

Enzymatic Nanosurgery *versus* Surgery with a Scalpel. We compared the efficacy of rats treated by nanoparticulate enzymatic surgery to rats that underwent traditional surgery with a scalpel. Collagenase-loaded liposomes were inserted into the gingival sulcus, and tooth alignment was evaluated using an orthodontic spring (Figure 3A−C).

Over a treatment period of 15 days, we measured a similar enhancement of the tooth alignment trajectory motion in rats that underwent a surgical procedure in which the supracrestal collagen fibers were sectioned with a scalpel and in rats that underwent the nanoenzymatic procedure. The nanoparticulate collagenase group had enhanced tooth alignment compared to both the sham group (empty liposomes) and the group treated with the free enzyme (Figure 3D). The liposomal nanoparticulate collagenase group also displayed a three-fold enhancement in tooth alignment compared to ordinary braces (Figure 3D). The accelerated tooth movement in the nanosurgery group compared to that in the other treatment

DOI: 10.1021/acsnano.7b07983
ACS Nano 2018, 12, 1482−1490

groups is attributed to the biological relaxation of the collagen fibers. After 15 days, the teeth reached their maximal magnitude of mobility and the orthodontic spring was removed. The improved *in vivo* activity of the nanoparticulate delivery system corroborates the rapid *in vitro* deactivation of the free enzyme (Figure 1E). This suggests that the liposomal systems protected the enzyme *in vivo*, prolonging its release profile and confined the spatial distribution of the enzyme to the treatment site (Figure 3E). The delivery system prevented the enzyme from deactivating prematurely and allowed it to maintain its therapeutic activity as compared to the free enzyme group.

Localized Biodistribution of the Enzymatic Nanosurgery Liposomes. One requirement a nanosurgery system must satisfy is specificity to the target site. This is achieved by selecting the proper proteolytic enzyme tailored biologically toward the target organ. In addition, the drug delivery system must confine the spatial biodistribution of the enzyme primarily to the treatment site and maintain the therapeutic dose needed for the surgery. To confine the release of collagenase to the treatment site, we tested the biodistribution of liposomes (100 nm) loaded with a fluorescent dye after being placed in the sulcus (Figure 3E). The nanoparticles remained in close vicinity of the treated tooth for 24 h. Eight hours post-administration, we found traces of the particles also around the tongue due to liposome leakage from the sulcus but not in the liver, heart, kidneys, or spleen (Figure 3E). Histological evaluation of these tissues demonstrated that they were unharmed (Figure 3F−O), most likely due to the collagenase deactivation in saliva (Figure 1E).

Aseptic inflammatory processes play a major role in preconditioning the alveolar bone for orthodontic tooth movement.[22] We compared the degree of inflammation in rats treated with ordinary orthodontics to those with orthodontics supplemented with nonencapsulated collagenase, liposomal collagenase, and surgery. Histological analysis of the gingival tissue shows similar presentation of mild inflammation among all groups (Figure 3F−O and Supplementary Figure S4).

Interestingly, the animals' eating pattern was minimally affected by the treatment. During the first week, all rats lost ∼10% of their body weight. A similar weight-loss profile occurs also in humans undergoing orthodontic treatments and is associated with adapting to a device in one's mouth. After completing the treatment, only the nanoparticulate enzymatic rats regained the weight they lost (Supplementary Figure S5). In comparison, rats treated by the traditional surgery displayed weight loss. Even though the teeth moved three-fold greater distance in the nanosurgery group, the rats continued eating solid pellet chow and regained normal weight, suggesting this treatment approach is associated with less discomfort.

Tissue Remodeling after Nanosurgery. Regeneration of the soft and hard tissues that surround the teeth is necessary after a surgical process. We observed the changes the alveolar bone underwent throughout the enzymatic process. For this, microCT scans of the maxillofacial bone were performed 15 days after initiating the treatment and 45 days after removing the braces (*i.e.*, day 60 of the experiment, Figure 3P−S). Interestingly, bone recovery was faster and to a greater extent in the nanoenzymatic group compared to bone repair in the group treated with ordinary braces. At the beginning of the procedure, in tandem with tooth movement, bone absorption was observed at the treatment site (Figure 3Q). On day 60 (45 days after removing the braces), full bone recovery was observed at the new tooth orientation (Figure 3S). These findings suggest that the periodontal bone regenerates in an improved manner after the nanoenzymatic surgical procedure.

Enzymatic Nanosurgery Reduces Tooth Relapse. Relapse is a condition in which the teeth shift out of alignment back to their preorthodontic treatment position. Approximately 40% of patients suffer relapse, usually leading to a second cycle of orthodontic treatment.[23] To avoid relapse, dentists affix the teeth using NiTi wires. Interestingly we noticed that nanosurgery treated rats had significantly less tooth relapse in comparison to the control group. On day 16 after removing the braces, the regular treatment completely relapsed, while the enzymatic nanoparticle treatment retained a 1 mm displacement gap at the treatment site (Supplementary Figure S6). We attribute the slow relapse in the nanoparticle-treated group to improved regeneration of the collagen fibers and bone at the target position.

CONCLUSIONS

Orthodontic procedures are prevalent among teenagers and adults. In many cases, a surgical intervention is necessary in order to maneuver the teeth to their proper position with braces.

Our goal was to develop a mode for performing biological, rather than physical, remodeling of connective tissue in the oral space. We demonstrate that controlled delivery of proteolytic enzymes using nanotechnology can replace minimal surgery.

Collagenase, a proteolytic enzyme with specificity toward collagen, plays a major role in remodeling the extracellular tissue matrix. Due to its degradative nature, collagenase has a short half-life and working distance *in vivo*, mitigating its effect only to its substrate.[24] Here, we harnessed collagenase, by integrating the enzyme into a drug delivery system, to degrade the supracrestal in a controlled manner. Specifically, liposomes, vesicles with an inner aqueous core surrounded by a lipid bilayer, were loaded with collagenase and applied to collagen fibers. At a therapeutic collagenase concentration of 0.05−0.16 mg/mL, the fibers relaxed but did not tear. The enzymatic treatment did not detach adherent fibroblasts from the collagen fibers. Moreover, secreted biomarkers indicated that the collagen was repaired by the fibroblasts. The repair was confirmed by the regeneration of the tensile strength and morphology of the collagen fibers over time.

When placed in the sulcus of rats (between the gingival tissue and the tooth), collagenase facilitated enhanced orthodontic tooth movement at three times the rate of ordinary braces. Histological sections of the treatment site demonstrated minor inflammation following the treatment. During the treatment, the animals did not lose weight, suggesting that despite the enhanced tooth motion the animals did not suffer increased oral pain that would prevent them from accessing chow.

Relapse, the return of teeth to their pretreatment orientation, is a major challenge in orthodontics. Reduced tooth relapse was observed after the braces were removed in the enzymatically treated group. This is attributed to soft and hard tissue remodeling at the new orientation rather than the return of the stressed teeth to their original orientation in the control group. CT scans during the therapeutic process and 45 days following the braces removal indicated that the underlying bone remodeled in the new orientation. Compared to traditional surgery, the enzymatic treatment achieved an improved outcome, had better recovery, and suggests less pain.

DOI: 10.1021/acsnano.7b07983
ACS Nano 2018, 12, 1482−1490

In summary, this study provides an approach for degrading connective tissue using proteolytic enzymes housed in nanoparticles rather than by surgical intervention. Combining nanotechnology and enzymatic drug delivery may prove effective in treating conditions where a tissue must be remodeled in a specific manner. This noninvasive procedure was shown to shorten the treatment time and improve recovery.

METHODS

Liposome Preparation. Collagenase type-I was incorporated into 100 nm liposomes. A lipid mixture of 1,2-dimyristoyl-*sn*-glycero-3-phosphocholine (Avanti Polar Lipids, Alabaster, Alabama), cholesterol (Sigma), and 1,2-distearoyl-*sn*-glycero-3-phosphoethanolamine-*N*-methoxy-polyethylene glycol 2000 (Avanti) in a molar ratio 56:39:5 was dissolved in 200 mL of 70% ethanol at 50 °C. The lipid mixture was hydrated in Dulbecco's phosphate buffer saline containing the collagenase (DPBS, Sigma-Aldrich, St. Louis, MO, USA) to reach a lipid concentration of 50 mM. The liposome dispersion was extruded at 45 °C using a high-pressure Lipex extruder (Northern Lipids, Vancouver, Canada) and sequential passaging through Nuclepore polycarbonate membrane membranes (Whatman, Newton, MA, USA) with a pore diameter of 800, 400, 200, and 100 nm. Five extrusion steps were applied per filter type. The average diameter size of the liposomes was determined by dynamic light scattering using a Zetasizer Nano ZSP (Malvern Instruments, UK). The mean size of the liposomes was 110−130 nm with polydispersity index of 0.04−0.09. The liposome solution was then dialyzed, using a 1×10^6 MWCO dialysis bag (SpectraPor Dialysis Membrane), against a phosphate-buffered saline solution for 24 h at 4 °C, exchanging the external media after 1, 3, and 24 h.

The encapsulated fraction of the collagenase was measured using microBCA assay following the dialysis process. The liposomes entrapped 8−10% of the initial amount of collagenase in the solution, resulting at ∼160−200 μg/mL in the liposomal dispersion, that is, 14−18 copies of encapsulated protein per liposome.

To load the enzyme without compromising its activity, a maximal working temperature of 50 °C, extrusion pressure of 10 bar, and ethanol content below 10% v/v were used (Supplementary Figure S7).

Cryo-TEM. Cryogenic temperature transmission electron microscopy (cryo-TEM) was used to image the liposomes, as described by Talmon.[25] We used an FEI Talos 200C, field emission gun equipped with a high-resolution TEM. The samples were mounted on Gatan 626 cryo-holders to maintain cryo-preservation in the TEM at −180 °C. Images were recorded with a FEI Falcon III camera, and the contrast was enhanced using a Volta Phase Plate.

Particle Biodistribution. Liposome biodistribution studies were performed on male Wistar rats using a whole animal Maestro *in vivo* imaging machine (Cambridge Research & Instrumentation, MA, USA); excitation = 671−705 nm, emission = 800 nm long pass, exposure time = 5000 ms.

Indocyanine green (ICG) was encapsulated in multilamellar liposomes by dissolving DMPC (Avanti Polar Lipids, Alabaster, AL), cholesterol (Sigma-Aldrich, St. Louis, MO), and DSPE-PEG (2000) (Avanti) in a 56:39:5 molar ratio in absolute ethanol. The lipid mixture was hydrated in phosphate-buffered saline containing 1.8 mg/mL ICG to form multilamellar liposomes. To produce unilamellar liposomes, the liposomes were extruded at 45 °C using a high-pressure Lipex extruder (Northern Lipids, Vancouver, Canada) and sequential passaging through Nuclepore polycarbonate membrane membranes (Whatman, Newton, MA, USA) with pore diameters of 800, 400, 200, and 100 nm. Five extrusion steps were applied per filter type. Nonencapsulated ICG was removed using a 1×10^6 MWCO dialysis bag (SpectraPor) against PBS at 4 °C for 24 h. The fluorescent liposomes were applied to five male Wistar rats on each side of the first upper molar, 50 μL to each side, and the animals were imaged before and 1, 4, 8, 12, and 24 h post-application. For each measurement, the rats were sacrificed, dissected, and the organs were imaged separately. Fluorescent intensity values were normalized to the highest signal in all organs and background was removed.

Thin Layer Chromatography (TLC). Liposomes, with or without collagenase, were dissolved in methanol, spot-loaded onto silica gel 60-F254 TLC plates (Merck), and placed in a TLC chamber with chloroform−methanol−water solution (75:20:5) as the mobile phase. The plate was held until the mobile phase reached a critical height, *versus* all four of their components separately: collagenase, cholesterol, PEG-2000, and DMPC.

Collagenase Activity Assay. Collagenase activity was assessed using fluorescein-conjugated gelatin (ThermoFisher) as a substrate. The enzyme solution was added to the substrate solution together with a reaction buffer (0.5 M Tris-HCl, 1.5 M NaCl, 50 mM $CaCl_2$, 2 mM sodium azide, pH 7.6). Fluorescence intensity for every sample was measured every 15 s for 3 min with excitation set at 485 nm and emission at 530 nm using the Infinite 200 PRO multimode reader (TECAN, Mannedorf, Switzerland). A linear incline was determined, and collagenase concentration was calculated using a calibration curve generated by collagenase samples of known concentrations.

Collagenase Release Assay. Collagenase release was assessed using a Micro BCA protein assay kit (Thermo Fisher Scientific, MA, USA). To separate between the encapsulated and released collagenase, the liposomal solutions for the different experimental time points (1−50 h) were ultracentrifuged for 45 min with the following parameters: 4 °C, 45 000 rpm. After the centrifugation, the supernatants were incubated with Triton X-100 diluted to 1% for 1.5 h at room temperature. Another 13 000 rpm centrifuge was done before the Micro BCA assay.

To test the collagenase activity, liposomal collagenase after dialysis or free collagenase in phosphate-buffered saline at a concentration of 5 μg/mL, was incubated at 37 °C. Every hour, a collagenase sample was assessed for its capacity to cleave a fluorescein-conjugated gelatin substrate (Thermo Fisher). Activity of the released collagenase was determined in accordance to the change in fluorescence over 3 min, relative to the fluorescence at $t = 0$.

Stress/Strength Profile of Collagen Fibers Exposed to Collagenase. Collagen type-I bundles, sourced from the tails of Wistar rats,[26] were suspended using a LLOYD LF-Plus digital material tester force machine. The bundles were suspended inside a bath loaded with a buffer that simulates the composition of the oral fluid: an isotonic solution, pH 6.7 at 37 °C complemented with electrolytes including sodium, potassium, calcium, magnesium, bicarbonate, and phosphates.[27] The bundles, 0.8−1.2 mm in diameter, were cut into two equal 4 cm sections, acting as an internal control. Collagenase type-I from *Clostridium histolyticum* (Sigma-Aldrich) was added at different concentrations, and the stress/strength profile of the collagen fibers was recorded as a function of the collagenase treatment. The ultimate tensile strength of the collagen bundle was determined for each collagenase concentration.

Fibroblast Adherence to Collagen Fibers. The fibroblast morphological change was recorded using the LSM 710 laser scanning confocal microscope (Zeiss) over a period of 90 min. The fibroblast nuclei were stained using Hoechst 33342 (Thermo Fisher Scientific, MA, USA). The Hoechast 16.23 mM stock solution was diluted 1:2000 in DPBS (Sigma-Aldrich, St. Louis, MO, USA), and the collagen fiber buffer was removed. Three microliters of the diluted solution was added, followed by 10 min light protected incubation. The staining solution was removed, and the fiber was washed three times in PBS.

Movie S1 of the fibroblasts morphological change can be seen at https://youtu.be/4krwecUS7Yc

Collagen Regeneration SEM. Collagen bundles were mounted on carbon tape and imaged using a Zeiss UltraPlus high-resolution scanning electron microscope equipped with an Everhart−Thornley secondary electron detector. Each bundle was cut in half. The untreated half acted as an internal control for each treated bundle. All data points are the mean of 14−20 experimental points. Collagen fibers were exposed to 0.05 mg/mL collagenase for 8 h. Ethylenediaminetetraacetic acid (EDTA; St. Louis, MO, USA), 3 mM along with two drops of NH_4Cl 1 M buffer, was added for 30 min in order to

DOI: 10.1021/acsnano.7b07983
ACS Nano 2018, 12, 1482−1490

retard the enzyme's activity. Subsequently, the medium was removed, and the treated bundles were washed two times with new growth media to allow bundle regeneration.

Collagen Fibers Regain Their Initial Mechanical Strength Post-nanosurgery. Collagen fibers were sourced from tails of Wistar rats. Each bundle was cut in half. The untreated half acted as an internal control for each treated bundle. All presented data points are the mean of 14−20 experimental points. Collagen fibers were exposed to collagenase at a concentration of 0.05 mg/mL for 8 h in order to weaken the bundles. After 8 h, a concentration of 0.02 M EDTA (St. Louis, MO, USA) was added for 15 min in order to inhibit the enzyme activity, hence allowing the bundle regeneration. Subsequently, the medium was removed, and the treated bundles were washed twice with new growth media.

RNA Extraction, PCR, and Real-Time PCR. mRNA was extracted from the rats' gingival tissue using a TRIzol reagent (Thermo Fisher Scientific, MA, USA). The mRNA sequences were first reverse-transcribed to complementary DNA with reverse transcriptase using a thermocycler (LabCycler SensoQuest PCR, SensoQuest, Germany). To quantify the genes, real-time PCR was employed (BioRad CFX96, Bio-Rad Laboratories Ltd., Israel). Each gene was independently amplified using specific probe and primers. Cycling times: 5 min at 95 °C (15 s at 95 °C, 45 s at 63 °C) × 40 cycles.

Tooth Displacement Model. All animal trials followed the Technion Institutional Ethical Committee's guidance. All rats were anesthetized in two stages. In the first stage, the rats were anesthetized with isoflurane. In the second stage, each rat was injected a mixture of ketamine and xylazine intraperitoneally. After each procedure, the rats were transferred and kept in an incubator, with constant oxygen flow, until they reached full recovery.

An ordinary orthodontic Ni−Ti closed coil spring (9 mm closed coil spring nickel and titanium alloy that has two eyelets with an inner radius of 0.76 mm) was used to connect the first molar in the upper pallet to the front upper incisors of the rat. The Ni−Ti coil spring was glued to the tooth (3 M UNITEK), generating a constant force of 200 G (1.96 N) when extended between 12 and 24 mm. The force applied in the oral cavity was the same on all the rats that participated in the experiment. This type of coil has been used and studied in orthodontics for years and has proven to be effective in orthodontic procedures. The procedure of installing the Ni−Ti coil closed spring was performed using human orthodontics equipment and materials. The first upper molar and the upper incisors were dried and cleaned using cotton swabs to remove any debris that accumulates. The teeth were conditioned using Transbond Plus etching primer conditioning agent by 3 M UNITEK for 5−10 s creating a rugged surface to allow for stronger bonding. Following the conditioning, a small amount of composite Transbond LR light-cure adhesive (3 M UNITEK) was spread over the molar. The eyelet ring of the Ni−Ti closed coil spring was placed in parallel with the tooth and light cured using LEDEX dental curing light for 10−15 s. Once again, a small amount of bonding agent was spread over the ring and light cured for at least 40 s. The binding of the incisors was performed in a similar manner. Cleaning, drying, and conditioning of the incisors were initially done. Subsequently, a stainless ligature was placed through the second eyelet ring of the Ni−Ti closed coil spring, and we were able to achieve strong binding by braiding it around the incisors.

Collagenase liposomes (see Liposome Preparation), or a similar concentration of free collagenase, were applied directly to the sulcus. To apply the formulations a 30 gauge needle was inserted carefully into the sulcus pocket, in a downward motion that was parallel to the tooth to a depth of ∼1−2 mm, and a 50 μL volume was deposited to the buccal and lingual side of the tooth. The total duration of the studies was 60 days: 15 days of braces with the different treatments and an additional 45 days of recovery (after the braces removal). During the 15 days of treatment, tooth displacement measurements were taken every 3 days using a digital caliper with an instrument error of 0.02 mm, and microCT scans were performed on day 15 and day 60. The distance between the eyelet of the Ni−Ti closed coil on the first molar and the back of the upper incisors was measured and recorded using the digital caliper. Before each tooth displacement measurement, the rats were weighed and then anesthetized using isoflurane. This kind of anesthesia allowed fast measurements and short recovery time for the rats.

Gd Liposomes. Diethylenetriaminepentaacetic acid gadolinium-(III) dihydrogen salt hydrate (Gd, Sigma) was loaded into 100 nm liposomes using the ethanol injection method.[28] Briefly, a lipid mixture of DMPC, cholesterol, and DSPE-PEG2000 at molar ratios of 56:39:5, respectively, was dissolved in absolute ethanol at 70 °C. Ethanol volume was 10% of the final liposome solution volume. The dissolved lipids were quickly injected into a PBS solution containing 0.271 mg/mL Gd to reach a lipid concentration of 50 mM. The liposomes were extruded five times through two 100 nm polycarbonate membranes (Whatman, USA) at 65 °C. Free Gd was removed by dialysis using a 12−14 kDa membrane (SpectraPor) against PBS solution at 4 °C for 24 h.

Gd−Liposome Biodistribution. Five male Wistar rats were applied 50 μL of the Gd liposomes in the rat's periodontal pocket. The rats were sacrificed 24 h after the liposomes placement, and the gingival tissue, skin, lungs, brain, spleen, urinary balder, kidneys, tongue, liver, stomach, and digestive system were collected. Tissues were combusted for 5 h at 550 °C and then dissolved in 1 vol % nitric acid. Gadolinium in each organ was quantified using ICP-EOS at wavelengths of 335.048 and 342.246 nm.

Histology. After the rats were sacrificed, the entire maxilla was extracted and kept in 10% natural buffer formalin at room temperature. Paraffin-embedded tumor blocks from the rat maxillas were prepared and sectioned in 4 μm thick slides and stained with hematoxylin/eosin (H&E). Axial and sagittal cuts from the upper jaw were observed.

CT Scans. Rats from the braces-only group and from the braces plus nanosurgery group were sacrificed, and the head and jaw were scanned using a Skyscan 1176 Micro-CT (Bruker, UK) equipped with an NRecon 1.6.9.8. at a 32 μm resolution under a 70 kV 355 μA source voltage, 90 ms exposure, and 0.8° rotation step.

Statistical Analysis. Data are presented as means ± SD. All statistical comparisons were performed using a two-tailed *t*-test for independent samples. A p value of <0.05 was considered to denote statistical significance. Singular factor ANOVA analysis was used among the tooth movement and the gene expression experiments to determine significantly difference. In addition, a Benjamini−Hochberg false discovery rate procedure was employed, using an error discovery rate of Q = 10% as a post hoc comparison test.[29]

ASSOCIATED CONTENT

Supporting Information

The Supporting Information is available free of charge on the ACS Publications website at DOI: 10.1021/acsnano.7b07983.

Thin layer chromatography of empty and collagenase-encapsulated liposomes (Figure S1); cryo-TEM images of collagenase-encapsulated liposomes (Figure S2); collagen fiber mechanical evaluation *ex vivo* stress/strain curves (Figure S3); histological inflammation assessment of the rat gingival tissue (Figure S4); body weight comparison between the surgery and nanosurgery groups (Figure S5); tooth relapse measurements, comparing the control and test groups *in vivo* (Figure S6); collagenase stability (Figure S7); collagen type-I activity profile at 4 °C for 6 h and the mechanical stress system characterization (Figure S8); and liposome biodistribution based on the Maestro CRI and elemental analysis results (Figure S9) (PDF)

AUTHOR INFORMATION

Corresponding Author

*E-mail: avids@technion.ac.il.

ORCID

Assaf Zinger: 0000-0001-7894-486X

DOI: 10.1021/acsnano.7b07983
ACS Nano 2018, 12, 1482−1490

Avi Schroeder: 0000-0003-2571-5937

Notes

The authors declare no competing financial interest.

ACKNOWLEDGMENTS

This study was supported by ERC-STG-2015-680242. The authors also acknowledge the Israel Ministry of Economy for a Kamin Grant (52752); the Israel Ministry of Science Technology and Space—Office of the Chief Scientist (3-11878); Israel Science Foundation (1778/13); Israel Cancer Association (2015-0116); German−Israeli Foundation for Scientific Research and Development for a GIF Young Grant (I-2328-1139.10/2012); European Union FP-7 IRG Program for a Career Integration Grant (908049); a Mallat Family Foundation Grant; Alon and Taub Fellowships to A.S.; Dr. Nitsan Dahan and Mrs. Yehudith Schmidet for their help during the scanning confocal and electron microscopy; Dr. Oscar Lichtenstein for his help with the *ex vivo* collagen stressing tests; Dr. R. Shofty, Dr. D. Levin-Ashkenazi, Ms. V. Zlobin, and Mr. N. Amit from the Technion Pre-Clinical Research Authority for their help with the *in vivo* animal tests; Ms. Bonnie Manor, Mr. Guy Nawi, Mr. Dima Zagorski, and Mr. Rohan Aggarwal for graphical aid; Ms. Shirley Pattisson for editing the manuscript; Merkel Technologies for their support in performing micro-CT scans. In addition, we thank Dr. E. Suss Toby, M. Holdengreber, and O. Schwartz from the Bioimaging Center at the Technion Faculty of Medicine for their assistance with imaging and image analysis.

REFERENCES

(1) Brown, J. L.; Nash, K. D. The Economics of Orthodontics. *American Association of Orthodontists Report*; San Francisco, CA, May 15−19, 2015.
(2) Nakashima, M.; Reddi, A. H. The Application of Bone Morphogenetic Proteins to Dental Tissue Engineering. *Nat. Biotechnol.* **2003**, *21*, 1025−1032.
(3) Vollenweider, M.; Brunner, T. J.; Knecht, S.; Grass, R. N.; Zehnder, M.; Imfeld, T.; Stark, W. J. Remineralization of Human Dentin Using Ultrafine Bioactive Glass Particles. *Acta Biomater.* **2007**, *3*, 936−943.
(4) Fernandez-Moure, J. S.; Evangelopoulos, M.; Colvill, K.; Van Eps, J. L.; Tasciotti, E. Nanoantibiotics: A New Paradigm for the Treatment of Surgical Infection. *Nanomedicine* **2017**, *12*, 1319.
(5) Vishwakarma, A.; Bhise, N. S.; Evangelista, M. B.; Rouwkema, J.; Dokmeci, M. R.; Ghaemmaghami, A. M.; Vrana, N. E.; Khademhosseini, A. Engineering Immunomodulatory Biomaterials to Tune the Inflammatory Response. *Trends Biotechnol.* **2016**, *34*, 470−482.
(6) Solomonov, I.; Zehorai, E.; Talmi-Frank, D.; Wolf, S. G.; Shainskaya, A.; Zhuravlev, A.; Kartvelishvily, E.; Visse, R.; Levin, Y.; Kampf, N.; Jaitin, D. A.; David, E.; Amit, I.; Nagase, H.; Sagi, I. Distinct Biological Events Generated by Ecm Proteolysis by Two Homologous Collagenases. *Proc. Natl. Acad. Sci. U. S. A.* **2016**, *113*, 10884−10889.
(7) Ghadiali, J. E.; Stevens, M. M. Enzyme-Responsive Nanoparticle Systems. *Adv. Mater.* **2008**, *20*, 4359−4363.
(8) Gilpin, D.; Coleman, S.; Hall, S.; Houston, A.; Karrasch, J.; Jones, N. Injectable Collagenase Clostridium Histolyticum: A New Non-surgical Treatment for Dupuytren's Disease. *Journal of hand surgery* **2010**, *35*, 2027−2038.
(9) Jang, H. L.; Zhang, Y. S.; Khademhosseini, A. Boosting Clinical Translation of Nanomedicine. *Nanomedicine* **2016**, *11*, 1495.
(10) Stark, W. J. Nanoparticles in Biological Systems. *Angew. Chem., Int. Ed.* **2011**, *50*, 1242−1258.
(11) Shilo, M.; Berenstein, P.; Dreifuss, T.; Nash, Y.; Goldsmith, G.; Kazimirsky, G.; Motiei, M.; Frenkel, D.; Brodie, C.; Popovtzer, R. Insulin-Coated Gold Nanoparticles as a New Concept for Personalized and Adjustable Glucose Regulation. *Nanoscale* **2015**, *7*, 20489−20496.
(12) Hafner, A.; Lovric, J.; Lakos, G.; Pepic, I. Nanotherapeutics in the Eu: An Overview on Current State and Future Directions. *Int. J. Nanomed.* **2014**, *9*, 1005−1023.
(13) Weissig, V.; Pettinger, T. K.; Murdock, N. Nanopharmaceuticals (Part 1): Products on the Market. *Int. J. Nanomed.* **2014**, *9*, 4357−4373.
(14) Peer, D.; Karp, J. M.; Hong, S.; Farokhzad, O. C.; Margalit, R.; Langer, R. Nanocarriers as an Emerging Platform for Cancer Therapy. *Nat. Nanotechnol.* **2007**, *2*, 751−760.
(15) Eliaz, R. E.; Szoka, F. C., Jr. Liposome-Encapsulated Doxorubicin Targeted to Cd44: A Strategy to Kill Cd44-Over-expressing Tumor Cells. *Cancer Res.* **2001**, *61*, 2592−2601.
(16) Brown, L. R. Commercial Challenges of Protein Drug Delivery. *Expert Opin. Drug Delivery* **2005**, *2*, 29−42.
(17) Nagase, H.; Woessner, J. F. Matrix Metalloproteinases. *J. Biol. Chem.* **1999**, *274*, 21491−21494.
(18) Wilson, J. J.; Matsushita, O.; Okabe, A.; Sakon, J. A Bacterial Collagen-Binding Domain with Novel Calcium-Binding Motif Controls Domain Orientation. *EMBO Journal* **2003**, *22*, 1743−1752.
(19) Reznikov, N.; Steele, J. A. M.; Fratzl, P.; Stevens, M. M. A Materials Science Vision of Extracellular Matrix Mineralization. *Nat. Rev. Mater.* **2016**, *1*, 16041.
(20) Mwenifumbo, S.; Stevens, M. M. ECM Interactions with Cells from the Macro-to Nanoscale. *Biomed. Nanostruct.* **2007**, 223−260.
(21) Harris, A. K.; Stopak, D.; Wild, P. Fibroblast Traction as a Mechanism for Collagen Morphogenesis. *Nature* **1981**, *290*, 249−251.
(22) Molinaro, R.; Corbo, C.; Martinez, J. O.; Taraballi, F.; Evangelopoulos, M.; Minardi, S.; Yazdi, I. K.; Zhao, P.; De Rosa, E.; Sherman, M. B.; De Vita, A.; Toledano Furman, N. E.; Wang, X.; Parodi, A.; Tasciotti, E. Biomimetic Proteolipid Vesicles for Targeting Inflamed Tissues. *Nat. Mater.* **2016**, *15*, 1037−1046.
(23) Johnston, C. D.; Littlewood, S. J. Retention in Orthodontics. *Br. Dent. J.* **2015**, *218*, 119−122.
(24) Brinckerhoff, C. E.; Plucinska, I. M.; Sheldon, L. A.; O'Connor, G. T. Half-Life of Synovial Cell Collagenase Mrna Is Modulated by Phorbol Myristate Acetate but Not by All-Trans-Retinoic Acid or Dexamethasone. *Biochemistry* **1986**, *25*, 6378−6384.
(25) Talmon, Y. The Study of Nanostructured Liquids by Cryogenic-Temperature Electron Microscopy—a Status Report. *J. Mol. Liq.* **2015**, *210*, 2−8.
(26) Rajan, N.; Habermehl, J.; Coté, M.-F.; Doillon, C. J.; Mantovani, D. Preparation of Ready-to-Use, Storable and Reconstituted Type I Collagen from Rat Tail Tendon for Tissue Engineering Applications. *Nat. Protoc.* **2007**, *1*, 2753−2758.
(27) Humphrey, S. P.; Williamson, R. T. A Review of Saliva: Normal Composition, Flow, and Function. *J. Prosthet. Dent.* **2001**, *85*, 162−169.
(28) Goldman, E.; Zinger, A.; da Silva, D.; Yaari, Z.; Kajal, A.; Vardi-Oknin, D.; Goldfeder, M.; Schroeder, J. E.; Shainsky-Roitman, J.; Hershkovitz, D.; Schroeder, A. Nanoparticles Target Early-Stage Breast Cancer Metastasis *in-Vivo*. *Nanotechnology* **2017**, *28*, 43LT01.
(29) Benjamini, Y.; Hochberg, Y. Controlling the False Discovery Rate: A Practical and Powerful Approach to Multiple Testing. *J. R. Stat. Soc. Ser. B* **1995**, 289−300.

DOI: 10.1021/acsnano.7b07983
ACS Nano 2018, 12, 1482−1490